Polymeric Tubulysin-Peptide Nanoparticles with Potent Antitumor Activity

Thomas Schluep,[1,2] Paula Gunawan,[1] Ling Ma,[1] Gregory S. Jensen,[1] Julienne Duringer,[1] Steven Hinton,[1] Wolfgang Richter,[3] and Jungyeong Hwang[1,2]

Abstract

Purpose: Tubulysins are naturally occurring tetrapeptides with potent antiproliferative activity against multiple cancer cell lines. However, they are also highly toxic in animal models. In order to improve the therapeutic index of this class of compounds, a nanoparticle prodrug of tubulysin A (TubA) was synthesized and evaluated *in vitro* and *in vivo*.

Experimental Design: A thiol derivative of TubA was covalently attached to a linear, β-cyclodextrin based polymer through a disulfide linker (CDP-TubA). The polymer conjugate assembled into stable nanoparticles. Inhibition of tubulin polymerization and antiproliferative activity of the polymer conjugate were evaluated *in vitro*. The preclinical efficacy of CDP-TubA administered i.v. was evaluated in nude mice bearing s.c. implanted human HT29 colorectal and H460 non – small cell lung carcinoma tumors.

Results: The IC_{50} of CDP-TubA (in Tub A equivalents) was 24, 5, and 10 nmol/L versus 3, 1, and 2 nmol/L for Tub A in NCI-H1299 (lung), HT-29 (colon), and A2780 (ovarian) cell lines, respectively. Tub A and the active thiol derivative were potent inhibitors of tubulin polymerization, whereas CDP-TubA showed minimal inhibition, indicating that target inhibition requires release of the peptide drug from the nanoparticles. The maximum tolerated dose of CDP-TubA was 6 mg/kg (in TubA equivalents) versus 0.05 mg/kg for TubA in nude mice. *In vivo*, a single treatment cycle of three weekly doses of CDP-TubA showed a potent antitumor effect and significantly prolonged survival compared with TubA alone.

Conclusions: Cyclodextrin polymerized nanoparticles are an enabling technology for the safe and effective delivery of tubulysins for the treatment of cancer.

There has been tremendously increased interest during the past few years in both synthesis (1–6) and potential cancer treatment applications (7–11) of compounds in the tubulysin family because of their potent antiproliferative activity against multiple cancer cell lines with IC_{50} in the nmol/L to pmol/L concentration range. Tubulysins are naturally occurring tetrapeptides isolated from strains of myxobacteria (12). Contrary to epothilones and taxol, which induce tubulin polymerization, they act as antimitotic agents that depolymerize cell microtubules and trigger apoptosis. Tubulysins bind to tubulin through the vinca site in a noncompetitive fashion with vinca alkaloids such as vincristine and vinblastine (8). Tubulysins are neither inhibitors of nor substrates for cytochrome P450 enzymes, which minimizes the potential for drug interactions (7). Tubulysins have also been found to be active in tumors that exhibit a multidrug resistance phenotype, especially in those with up-regulated surface p-glycoprotein pumps (7). Total synthesis of multiple tubulysin analogs and accompanying structure-activity relationship studies have revealed several analogs with equal or greater activity compared with the natural compounds that are both easier to synthesize and also more stable under physiologic conditions (1, 13).

However, despite all the aforementioned attractive characteristics, the pharmaceutical development of tubulysins has been hampered by their remarkably high toxicity and low solubility. One way to overcome these issues common to many cytotoxics is targeted delivery of compounds to cancer tissues. Strategies commonly used for this purpose are liposomal encapsulation (14, 15), conjugation to antibodies or small molecules targeted to antigens that are up-regulated in certain cancer types (16, 17), and polymer conjugation (18, 19). The use of macromolecular carriers and nanoparticles in this setting is based on their ability to positively change the pharmacokinetics and pharmacodynamics of chemotherapeutics by (*a*) enhancing solubility and therefore reducing third-spacing, (*b*) increasing circulation half-life by avoiding first-pass kidney clearance, (*c*) protecting drugs from enzymatic degradation, (*d*) increasing drug concentration in the tumor by the enhanced permeability and retention effect, (*e*) controlling release kinetics to more closely match the mode of action of these drugs, and (*f*) overcoming multidrug

Authors' Affiliations: [1]Insert Therapeutics and [2]Calando Pharmaceuticals, Pasadena, California; and [3]R&D Biopharmaceuticals, Martinsried, Germany

Received 7/16/08; revised 9/12/08; accepted 9/19/08.

The costs of publication of this article were defrayed in part by the payment of page charges. This article must therefore be hereby marked *advertisement* in accordance with 18 U.S.C. Section 1734 solely to indicate this fact.

Note: Supplementary data for this article are available at Clinical Cancer Research Online (http://clincancerres.aacrjournals.org/).

Requests for reprints: Thomas Schluep, Calando Pharmaceuticals, 129 N. Hill Avenue, Suite 104, Pasadena, CA 91106. Phone: 626-783-7200; Fax: 626-683-7220; E-mail: tschluep@calandopharma.com.

doi:10.1158/1078-0432.CCR-08-1848

Translational Relevance

Tubulin-targeted drugs are the mainstay of current cancer treatments, but many patients eventually still progress due to the rise of resistance and side effects leading to dose reductions or discontinuations. There is a great unmet need for new therapies that can overcome resistance and are better tolerated. Tubulysins are a novel tubulin-targeted class of natural compounds that are highly active in multidrug-resistant cells. However, natural tubulysins are also highly toxic in animal models and have no therapeutic window. Here we report for the first time on the synthesis, *in vitro* and *in vivo* evaluation of a nanoparticle produg of tubulysin A. This prodrug approach dramatically increases the tolerability of tubulysin A, resulting in a therapeutic index similar to or greater than currently approved tubulin inhibitors. We believe that nanoparticle conjugation may enable the clinical development of this class of compounds as potent anticancer agents.

resistance by intracellular delivery through endocytosis rather than diffusion, a process that is less susceptible to surface pump–mediated multidrug resistance. We have previously reported that conjugation of another cytotoxic drug, camptothecin, to a linear, β-cyclodextrin (β-CD)-based polymer (CDP) can increase the solubility and improve the biodistribution to tumor tissue compared with the parent compound administered by itself (20). Preclinically, this resulted in increased efficacy and reduced toxicity compared with camptothecin and irinotecan, a small molecule analog of camptothecin (21, 22). In humans, the CDP-camptothecin conjugate IT-101 showed excellent tolerability and promising signs of early clinical activity in heavily pretreated patients with solid tumors (23).

In CDP-TubA, a thiol derivative of the natural compound tubulysin A (TubA) is linked to CDP through a disulfide bond (Supplementary Fig. S1). A disulfide bond containing linker was chosen among various covalent linkages because of its reported high plasma stability and selective release characteristics. It takes advantage of a high redox potential difference between the oxidizing extracellular environment and the reducing intracellular space to become a selective delivery tool (24). Disulfide prodrugs have been reported to release their payload after uptake by cells through endocytosis. Disulfide linkers have gained more and more attention in drug formulations and delivery especially in macromolecular drugs such as antibody-drug conjugates that are targeted to internalizing surface ligands (25–28). CDP-polymer conjugates have also been shown to be taken up by cancer cells through endocytosis (29).

Here we report for the first time on the synthesis of CDP-TubA, a series of *in vitro* studies on CDP-TubA including IC_{50}, release and tubulin inhibition studies, and subsequent *in vivo* studies including maximum tolerated dose (MTD) and efficacy studies in two mouse tumor xenografts.

Materials and Methods

General

All of the anhydrous solvents, high performance liquid chromatography (HPLC) grade solvents, and other common organic solvents were purchased from commercial suppliers and used without further purification. Parent polymer, Poly-CD-PEG, was synthesized as previously described (20). The polymer conjugate with methylprednisolone (CDP-MP) was synthesized as previously described (30). TubA was isolated and purified from the myxobacterium *Archangium gephyra* as previously described (10). The purity of TubA was 97.1% by HPLC, and identity was confirmed by electron spray mass spectrometry (m/z expected 843.45; found 843.8). Paclitaxel was purchased from Natural Pharmaceuticals, Inc. Vinblastine was from American Pharmaceutical Partners. Human plasma was purchased from Sigma. NMR spectra were recorded on a Varian 300 MHz spectrometer. Mass spectral analysis was done on Thermo Finnigan electrospray mass spectrometer, LCQ DECA (Thermo Fisher Scientific). Molecular weights of the polymer samples were analyzed on a Wyatt WinGPC Unity system coupled with double gel permeation columns (PL-aquagel-OH-40, 8 μm, 300 × 7.5 mm, Polymer Laboratories) on HP 1100 HPLC system (Agilent). TubA, TubA derivatives, and polymer-TubA conjugates were analyzed with a C-18 reverse phase column (Synergi Hydro-RP, 4 μm, 250 × 4.6 mm, Phenomenex) on a HP 1100 HPLC system using ammonium bicarbonate buffer (pH 8) and acetonitrile. Particle size measurement by dynamic light scattering was done on a ZetaPALS instrument (Brookhaven Instruments).

Synthesis of Poly-CD-PEG-SS-Py, 1

A mixture of parent polymer, Poly-CD-PEG (70 KD, 2 g, 0.43 mmol), pyridine dithioethylamine hydrochloric salt (384 mg, 1.73 mmol), N-(3-dimethylaminopropyl)-N′-ethylcarbodiimide hydrochloride (EDC; 333 mg, 1.73 mmol), and N-hydroxysuccinimide (NHS; 198 mg, 1.73 mmol) were dried overnight under vacuum (Supplementary Fig. S2). Then anhydrous N,N-dimethylformamide (DMF; 40 mL) was added to the mixture followed by anhydrous N,N-diisopropylethylamine (DIEA; 0.3 mL, 1.73 mmol). The reaction mixture was stirred under argon at room temperature for 4 h. Diethyl ether (300 mL) was then added into the mixture to precipitate the polymer. The crude product was dissolved in H_2O (400 mL) and the solution was dialyzed using a 25,000 MWCO membrane (Spectra/Por 7, Spectrum Laboratories) against water, filtered through a 0.2-μm filter membrane and lyophilized to yield 1.64 g of Poly-CD-PEG-SS-Py (82% yield) as a white solid.

Table 1. IC_{50} of TubA, CDP-TubA, 2-mercaptoethyl amide of TubA, and TubA-SS-TubA in human HT29 colorectal, human A2780 ovarian, and human H1299 non–small cell lung carcinoma cells

Cell line	TubA (nmol/L)	CDP-TubA (nmol/L)	2-mercaptoethyl amide of TubA (nmol/L)	TubA-SS-TubA (nmol/L)
HT29	1.3	4.9	4.4	2.5
A2780	1.6	9.7	8.7	4.1
NCI-H1299	2.8	23.7	19.0	6.6

NOTE: All IC_{50} values were acquired in a 48 h MTS assay and are expressed in tubulysin monomer equivalents.

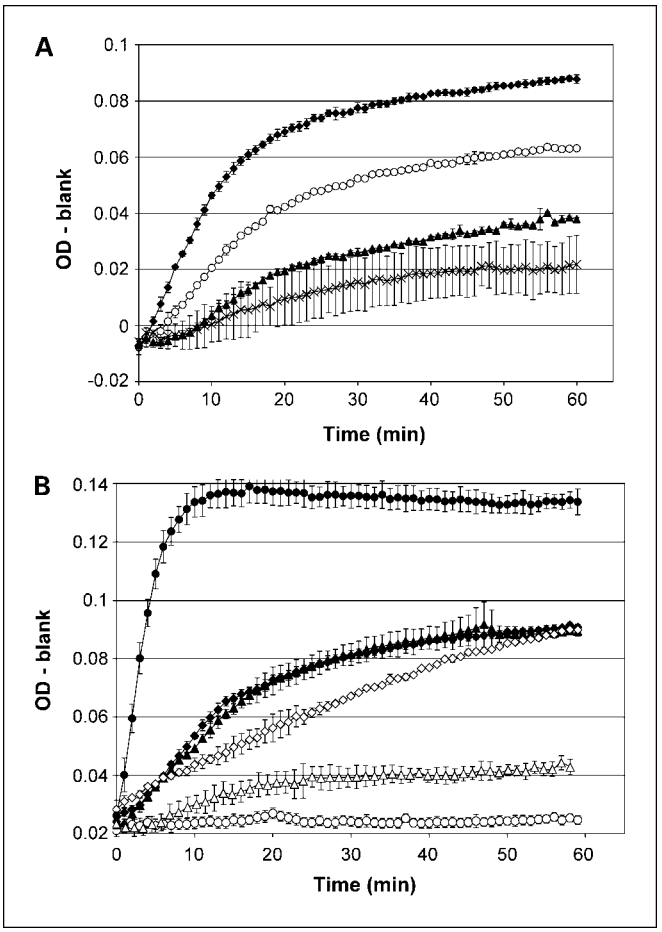

Fig. 1. Influence of TubA and CDP-TubA on tubulin polymerization *in vitro. A,* purified tubulin protein (30 μmol/L) was polymerized at 32°C in the presence of increasing concentrations of TubA. Polymerization was monitored by measuring optical density at 360 nm. (♦ untreated tubulin, ○ 2.5 μmol/L TubA, ▲ 6.25 μmol/L TubA, × 10 μmol/L TubA). *B,* polymerization of tubulin in the presence of CDP-TubA (◇, 10 μmol/L) and its active component, TubA-SH (Δ, 10 μmol/L). Controls included untreated tubulin (♦), a polymer conjugate of methylprednisolone (▲, 10 μmol/L), TubA (○, 10 μmol/L), and paclitaxel (●, 10 μmol/L). All concentrations are in active drug equivalents (TubA or methylprednisolone).

Synthesis of Poly-CD-PEG-SH, 2

To a PBS (6.8 mL) solution of Poly-CD-PEG-SS-Py (155 mg, 0.032 mmol) was added a solution of DTT in water (1 mL, 0.64 mmol; Supplementary Fig. S2). The reaction mixture was stirred at room temperature for 3 h and then dialyzed directly by a 25K MWCO membrane in degassed EDTA (1 mmol/L, 2 L) in water. After filtration through a 0.2-μm filter membrane, the solution was lyophilized to produce a white solid (109 mg) in quantitative yield.

Synthesis of pyridin-2-yldisulfanyl ethyl amide derivative of TubA, 3

To a solution of pyridine dithioethylamine hydrochloric salt (15.8 mg, 0.071 mmol) in anhydrous DMF (1.5 mL) was added DIEA (25 μL, 0.142 mmol) followed by a solution of tubulysin A (40 mg, 0.047 mmole) in anhydrous DMF (0.5 mL) and O-Benzotriazole-N,N,N′,N′-tetramethyl-uronium-hexafluoro-phosphate (HBTU; 0.047 mmol; Supplementary Fig. S2). The reaction mixture was stirred under argon at room temperature for 2 h. The mixture was then evaporated under vacuum. The crude product was purified by silica gel column chromatography (CH_2Cl_2/MeOH, 15/1) to afford white solid (54 mg) in 90% to quantitative yield. Purity was >99% by HPLC and identity was confirmed by electron spray mass spectrometry (m/z expected 1012.35; found 1034.80 M + Na).

Synthesis of Poly-CD-PEG-SS-TubA (CDP-TubA)

Poly-CD-PEG-SH (43 mg, 0.0094 mmole) was dissolved in degassed MeOH (1.8 mL), into which was added a methanol solution (0.35 mL) of 3 (9.5 mg, 0.0094 mmole) to bring the total reaction volume of 2.15 mL (Supplementary Fig. S2). The resulting yellow mixture was stirred under argon at room temperature for 4 h. N-ethyl maleimide

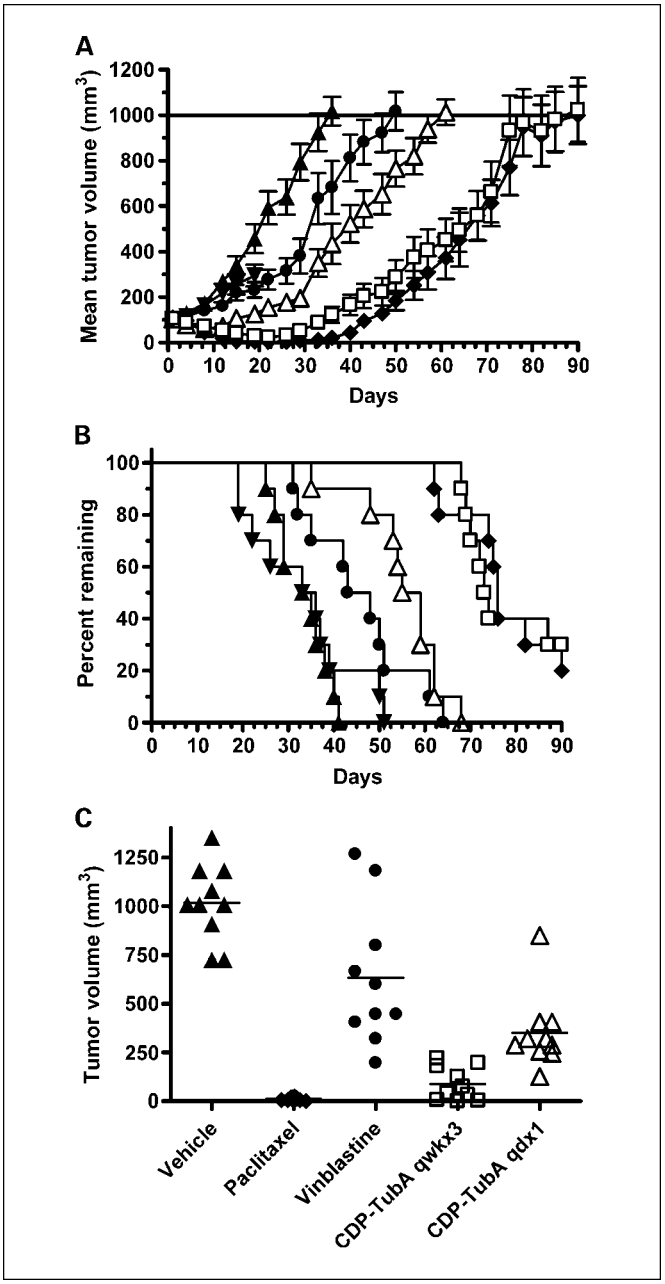

Fig. 2. Efficacy study in nude mice bearing s.c. human HT29 colorectal tumors. Animals were treated i.v. with vehicle (▲), free TubA (▼, 0.1 mg/kg qwk × 3), vinblastine (●, 4 mg/kg qwk × 3), paclitaxel (♦, 30 mg/kg qod × 5), CDP-TubA (Δ, 3 mg/kg qd × 1), or CDP-TubA (□, 3 mg/kg qwk × 3). *A,* mean tumor growth curves. Bars, SE. *B,* Kaplan-Meier survival plot for animals remaining in the study. *C,* tumor volume on the day the mean tumor volume of the vehicle control group reached the predetermined endpoint of 1,000 mm^3 (day 33). Qd, single dose; qwk, weekly; qod, every other day; all doses in tubulysin equivalents.

Table 2. Antitumor activity of CDP-TubA in the HT29 human colorectal carcinoma xenograft model in nude mice

Group	Treatment regimen			Median	T-C	%TGD	Statistical significance*		
	Agent	mg/kg	Schedule	TTE			vs G1	vs G5	vs G6
1	Vehicle	-	qwk ×3	33.6	—	—	—	‡	‡
2	Tubulysin	0.1	qwk ×3	34.5	0.9	3	ne	ne	ne
3	Paclitaxel	30	qod ×5	76.3	42.7	127	‡	ns	‡
4	Vinblastine	4	qwk ×3	45.1	11.5	34	§	‡	ns
5	CDP-TubA	3	qwk ×3	73.5	39.9	119	‡	—	‡
6	CDP-TubA	3	qd ×1	56.9	23.3	69	‡	‡	—

NOTE: Potency was evaluated using log-rank testing on the time it took for individual tumors to reach a predetermined endpoint (TTE) of 1,000 mm^3 and by comparing the mean tumor volume (MTV) for different treatment groups when tumors of vehicle-treated animals reached 1,000 mm^3 (day 33). Ten animals per group were treated. CDP-TubA (batch #1) doses are in tubulysin equivalents.
Vehicle, 10% DMSO: 1% Tween 80 in saline.
T-C, difference between median TTE (d) of treated versus control group; %TGD, [(T-C)/C] × 100.
MTV, mean tumor volume ± SD (mm^3) on the day the vehicle control group mean tumor volume reached the predetermined endpoint of 1,000 mm^3.
Mean BW nadir, lowest group mean body weight, as % change from Day 1; —, no decrease in mean body weight was observed.
Abbreviations: PR, partial regressions; CR, total number complete regressions; TFS, tumor-free survivors, i.e., CRs at end of study; TR, treatment-related; ne, not evaluable; ns, not significant.
*Statistical significance, Log-rank test.
†Statistical significance, ANOVA w. Tukey's post test.
‡$P < 0.001$.
§$P < 0.01$.
‖$P < 0.05$.

(118 mg, 0.94 mmol) was then added to quench the reaction resulting in clear, colorless solution. This solution was dialyzed using a 25K MWCO membrane, filtered through a 0.2-μmfilter membrane and lyophilized to afford CDP-TubA (27 mg, 45% yield) as a white solid. Loading was determined by HPLC to be 12% w/w and 16% w/w for the two batches prepared (Supplementary Table S1).

Determination of wt% ethyl thiol (2-mercaptoethyl amide) of TubA (TubA-SH) on the conjugates

A stock solution of CDP-TubA was prepared at a concentration of 10 mg/mL in water. An aliquot of this stock solution was diluted to 1 mg/mL with starting mobile phase, a mixture of 70% acetonitrile and 30% ammonium bicarbonate. To this an equal volume of freshly prepared DTT (200 mmol/L) in starting mobile phase was added. The mixture was incubated for 30 min at room temperature to allow for the reaction to go to completion. Twenty microliters of the incubated mixture were injected to an HPLC, and TubA-SH was determined at 254.4 nm with a gradient method. The TubA-SH peak area was integrated and compared with a standard curve to obtain the loading.

Release of TubA-SH from conjugates

Release of TubA-SH in PBS. CDP-TubA was dissolved in PBS (pH 7.4) or PBS acidified with 1N HCl (pH 5.5) at a concentration of 3 mg/mL. Aliquots (50 μL) were incubated at 37°C and at selected time points samples were placed at -80°C until analysis. For the released amount of TubA-SH, an equal volume of mobile phase was added and samples were analyzed by HPLC. For the total amount of polymer bound TubA-SH, an equal volume of 200 mmol/L DTT in mobile phase was added, stirred for 1 h, and analyzed by HPLC as described above.

Release of TubA-SH in human plasma. CDP-TubA was dissolved in PBS (pH 7.4) at a concentration of 3 mg/mL. Human plasma was prepared at a concentration of 1 mg/mL in water. An equal volume of the polymer conjugate solution (75 μL) and the human plasma were mixed, incubated at 37°C, and at selected time points samples were placed at -80°C until analysis. For the released amount of TubA-SH, samples were treated with methanol (225 μL) and mobile phase (75 μL) to precipitate out proteins. Samples were centrifuged to remove the precipitate, and the supernatant was analyzed. For the total amount of polymer bound TubA-SH, 200 mmol/L DTT (75 μL) in mobile phase were added and stirred for 1 h. Methanol (225 μL) was added to precipitate out proteins. Samples were centrifuged to remove the precipitate, and the supernatant was analyzed. The amount of released TubA-SH and the total amount of polymer bound TubA-SH were determined by HPLC as described above.

Tubulin polymerization assay

The tubulin polymerization assay was done according to the manufacturer's instructions with minor modifications (HTS-Tubulin Polymerization Assay Kit, Cytoskeleton, Inc.). Briefly, varying amounts of test compound were added to tubulin heterodimer (final concentration of 30 μmol/L dimer) in cold assay buffer containing 80 mmol/L PIPES, pH 6.9, 2 mmol/L $MgCl_2$, 0.5 mmol/L EGTA, 10% glycerol, and 1 mmol/L GTP. Solutions were immediately placed in a spectrophotometer at 32°C and optical density (OD, absorbance at 360 nm) recorded over time. Inhibition of tubulin polymerization was determined by comparing the maximum polymerization velocity (maximum slope of OD versus time) and increase in end point OD at 60 min with untreated control reactions.

Immunocytochemistry

A2780 human ovarian carcinoma cells were obtained from the American Type Culture Collection. Cells were grown on tissue chamber slides in RPMI 1640 containing 10% fetal bovine serum at 37°C for 24 h in a humidified 5% CO_2 atmosphere. Cells were exposed to media containing the tubulin inhibitor of interest for 5 h under the same conditions. Cells were then removed from the incubator, washed with PBS, fixed with cold methanol/acetone (1:1, -20°C) for 10 min, and incubated for 20 min with 10% normal goat serum in PBS to block unspecific absorption. Cells were further incubated with a mouse anti-α-tubulin antibody (1:1000, T6199, Sigma-Aldrich), washed with PBS, stained with a goat antimouse FITC antibody (1:250, sc-2010, Santa Cruz), washed again, and counter stained with 4′-6-Diamidino-2-phenylindole (DAPI). Images were acquired at a 100× magnification on a Zeiss 410 laser scanning microscope (Carl Zeiss) using two-photon excitation at 720 nm for DAPI, single photon excitation at 488 nm for

Table 2. Antitumor activity of CDP-TubA in the HT29 human colorectal carcinoma xenograft model in nude mice (cont'd)

MTV	Statistical significance †			Regressions			Mean BW nadir	TR deaths
Day 33	vs G1	vs G5	vs G6	PR	CR	TFS		
1018 ± 198	—	‡	‡	0	0	0	—	0
651 ± 59.5	ne	ne	ne	0	0	0	-26.8% Day 26	5
11 ± 8.1	‡	ns	§	1	9	1	-10.2% Day 12	0
633 ± 357	‡	‡	‖	0	0	0	-3.6% Day 4	0
88.1 ± 85.8	‡	—	‖	6	3	1	-2.2% Day 4	0
350 ± 193	‡	‖	—	0	0	0	-2.9% Day 4	0

FITC, and emission filters of 390 to 465 nm and >505 nm (long pass filter) for DAPI and FITC, respectively.

IC_{50} via MTS assay

The human ovarian carcinoma A2780, colorectal adenocarcinoma HT29, and lung carcinoma NCI-H1299 cells were obtained from the American Type Culture Collection. Cells were seeded in 96-well plates at a concentration of 5,000 cells per well and grown in medium containing 10% fetal bovine serum at 37°C for 24 h in a humidified 5% CO_2 atmosphere. The medium was replaced with fresh medium containing the test compounds at concentrations ranging from 0.01 nmol/L to 1 μmol/L. Triplicate wells per plate were treated at each concentration. Controls were vehicle-treated cells and medium only blank. Plates were incubated at 37°C for 48 h. MTS assay reagent was prepared by diluting CellTiter 96 AQueous One Solution (Promega) 5-fold into PBS/glucose (4.5 g/L). Cell culture medium was aspirated and 100 μL of MTS reagent were added to each well. Plates were incubated at 37°C for 1 to 2 h depending on the cell line. The plates were shaken for 5 min and the absorbance was measured at 485 nm using a SPECTRAFluor Plus plate reader (Tecan). The percentage of cell survival was calculated relative to untreated cells, and IC_{50}s were estimated from the graphs of log dose (nmol/L) versus % cell survival (GraphPad Prizm).

Animal care

All mice were housed in a pathogen-free animal facility at Piedmont Research Center according to the Guide for Care and Use of Laboratory Animals and the regulations of the Institutional Animal Care and Use Committee. The animal program at Piedmont Research Center is accredited by the Association for Assessment and Accreditation of Laboratory Animal Care.

Subcutaneous human tumor xenografts

HT29 colon carcinoma and NCI-H460 non–small cell lung carcinoma cell lines were from the American Type Culture Collection. HT29 cells were maintained in female athymic nude mice (*nu/nu*, Harlan) whereas H460 non–small cell lung carcinoma cells were grown in RPMI-1640 medium containing 10% heat inactivated fetal bovine serum, 100 units/mL penicillin G sodium, 100 μg/mL streptomycin sulfate, 25 μg/mL gentamicin, 2 mmol/L glutamine, 10 mmol/L HEPES, 0.075% sodium bicarbonate, and 1 mmol/L sodium pyruvate. Then 1 mm^3 tumor fragments (HT29) or 1×10^7 cells in 0.2 mL PBS (H460) were implanted s. c. into the right flank of each test mouse. Tumors were measured in two dimensions with calipers biweekly to the end of the study. When tumors reached an average size of 80 to 120 mm^3 for HT29 and 100 to 200 mm^3 for H460, a pair match was done to sort mice into groups of ten each and then treatment was started (day 1). All of the treatments were given i.v. The end point of the experiment was a tumor volume of 1,000 mm^3 or 90 d for HT29, and 2,000 mm^3 or 50 d for H460. When the tumor reached the end point the mouse was euthanized and the end point tumor growth delay was calculated consequently. End point tumor size was prospectively chosen to maximize the number of tumor doublings within the exponential growth phase in the control animals.

Determination of treatment efficacy

Treatment efficacy was determined by the time it took a specific tumor to reach the predetermined end point size and by comparing tumor volumes between treatment groups when the mean tumor size of vehicle control animals reached the predetermined endpoint size.

The time to end point (TTE) for each mouse was calculated as previously described (21). Partial regression response is defined as a tumor volume ≤50% of its day 1 volume for three consecutive measurements during the course of the study and ≥13.5 mm^3 for one or more of these three measurements. Complete regression response is defined as a tumor volume <13.5 mm^3 for three consecutive measurements during the course of the study. A tumor-free survivor is an animal with a complete regression response at the end of the study.

Determination of tolerability

Animals were weighed daily on days 1 to 5, then twice per week until the completion of the study. The mice were examined for overt signs of any adverse drug-related side effects. Acceptable toxicity for the MTD was defined as group mean weight loss of <20% or ≤10% animal deaths from toxicity.

Statistical and graphical analyses

The log-rank test was applied to analyze the significance of the difference between the TTE value distributions of two groups. The two-tailed statistical analyses were conducted at $P = 0.05$. The final tumor size recorded for the mouse was included with the data used to calculate the mean tumor size at subsequent time points when a mouse exited the study due to tumor size or treatment-related death. Tumor volume comparisons between groups were done by one-way ANOVA using a Tukey's post test.

Results

Synthesis of CDP-TubA conjugates. The conjugate was synthesized in a four-step synthesis starting from Poly-CD-PEG, the parent polymer, and TubA (Supplementary Fig. S2). Pyridin-2-yldisulfanyl ethyl amide derivative of both TubA, step 3, and β-cyclodextrin based polymer, step 1, were synthesized by a standard peptide conjugation method using conjugating agents such as HBTU and EDC with high yields. After DTT treatment of step 1, the free thiol containing polymer, step 2, was purified by dialysis in argon-purged EDTA water solution to prevent the sulfhydryls from spontaneous auto-oxidization in air to form disulfide bonds intramolercularly or intermolecularly. Step 2 was then applied to react with step 3 in a ratio of one repeat unit of polymer to one molar equivalent of step 3 to form the disulfide conjugate. Because each repeat unit on step 2 has two free thiols available, the remaining thiols were then quenched with N-ethyl maleimide. The theoretical wt% loading of 2-mercaptoethyl amide of TubA is 31.2% with the ratio of one molar repeat unit on step 2 to two molar equivalents of

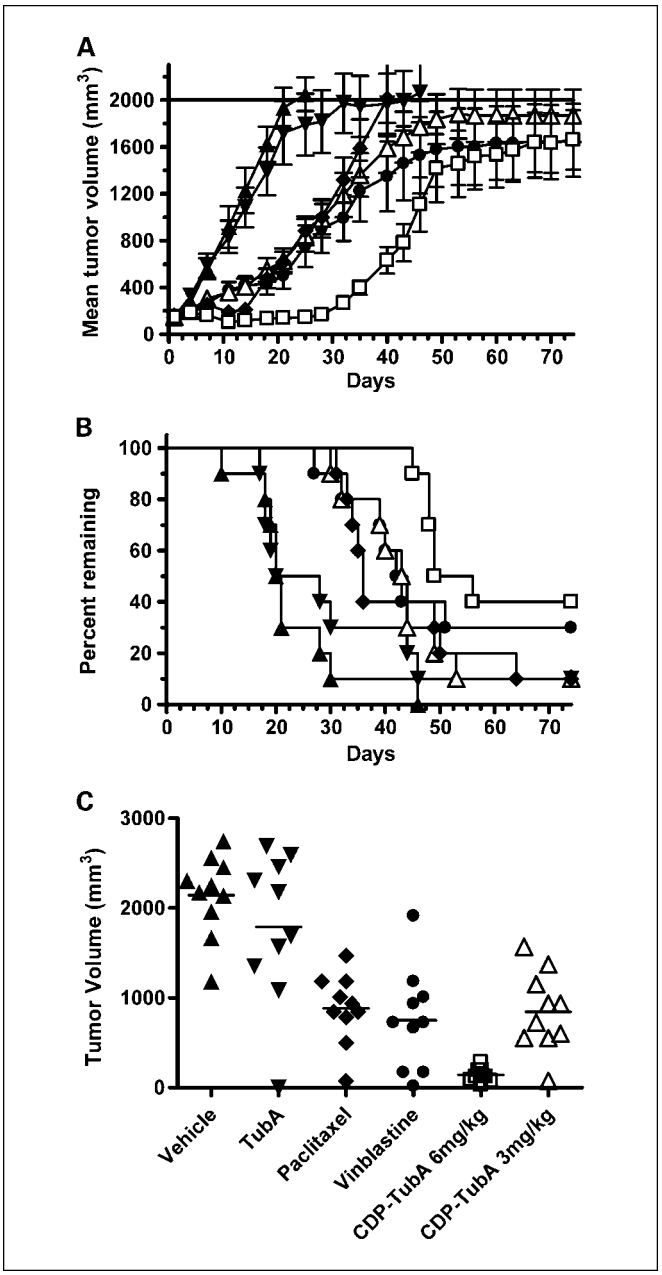

Fig. 3. Efficacy study in nude mice bearing s.c. human H460 non – small cell lung carcinoma tumors. Animals were treated i.v. with vehicle (▲), free TubA (▼, 0.025 mg/kg qwk × 3), vinblastine (●, 8 mg/kg qwk × 3), paclitaxel (♦, 30 mg/kg qod × 5), CDP-TubA (Δ, 3 mg/kg qwk × 3), or CDP-TubA (□, 6 mg/kg qwk × 3). *A,* mean tumor growth curves. Bars, SE. *B,* Kaplan-Meier survival plot for animals remaining in the study. *C,* tumor volume on the day the mean tumor volume of the vehicle control group reached the predetermined endpoint of 2,000 mm^3 (day 25).

step 3. The weight percent loading of TubA on polymer can be controlled through changing the ratio between steps 2 and 3, and we have synthesized polymer conjugates with a wt% loading ranging from 2% to 28%.

Two batches of conjugate were prepared and characterized by HPLC and dynamic light scattering (Supplementary Table S1). Although the parent polymer had a mean particle size of approximately 8 nm by dynamic light scattering, the polymer conjugates had a mean particle size of 100 to 130 nm and a relatively wide size distribution (half-width 50-80 nm). Solubility of TubA in water was approximately 0.1 mg/mL at neutral pH whereas that of CDP-TubA was at least 10 mg/mL in TubA equivalents (>100 mg/mL CDP-TubA). The CDP-TubA conjugate was stable for >6 months without any change in characteristics or purity when stored as a lyophilized solid at -20°C.

Release of tubulysin from CDP-TubA conjugate. The release of tubulysin from the polymer conjugate was studied at 37°C in PBS (pH 7.4) and human plasma (pH 7.4). Minimal release of <0.5% was seen in both conditions over 72 hours (data not shown). As expected, the released species detected were predominantly the 2-mercaptoethyl amide of TubA (TubA-SH) and its dimer (TubA-SS-TubA). Additionally, at 48 and 72 hours two unidentified degradation products were detected at low levels (<0.15%). This indicates that the polymer conjugate was stable in physiologic conditions for extended periods of time. Release was even lower at reduced pH (PBS adjusted to pH 5.5 with HCl), confirming that the disulfide cleavage is a redox and not a pH-driven process.

IC_{50} measurement by MTS assay. The cytotoxicity of TubA, CDP-TubA, 2-mercaptoethyl amide of TubA, and the TubA-SS-TubA dimer was tested in the HT29 colorectal, A2780 ovarian, and NCI-H1299 non – small cell lung carcinoma cell lines using an MTS assay (Table 1). The IC_{50} of TubA was in the low nmol/L range. The IC_{50} values of CDP-TubA were four to eight times higher than that of TubA. Interestingly, the IC_{50} values of both CDP-TubA and 2-mercaptoethyl amide of TubA were very similar to each other. The TubA-SS-TubA dimer was approximately two to three times more potent than the corresponding monomer containing the free sulfhydryl, when potency was expressed in tubulysin monomer equivalents.

Tubulin inhibition. Inhibition of tubulin polymerization by TubA was studied in a cell-free system (Fig. 1A). TubA showed a dose-dependent inhibition of polymerization of tubulin (30 μmol/L concentration) with an IC_{50} of 3.2 μmol/L and 5.4 μmol/L depending on whether maximum polymerization velocity or end point OD, respectively, was used to calculate potency (Supplementary Table S2).

In a separate experiment, tubulin polymerization was studied in the presence of the polymer conjugate CDP-TubA and the active derivative, TubA-SH (Fig. 1B, Supplementary Table S3). The CDP-TubA polymer conjugate affected the polymerization kinetics, suppressing the maximum polymerization velocity, but did not affect the end point OD at 60 minutes. A polymer conjugate with methylprednisolone, a steroid that is not known to bind to tubulin, did not affect the polymerization of tubulin, indicating that the effect on polymerization kinetics is mediated by the tubulysin component of the conjugate. The free thiol derivative TubA-SH was significantly more potent than the conjugated form, reducing both the maximum polymerization velocity and end point OD (Supplementary Table S3). The most potent tubulin polymerization inhibitor in this experiment was TubA, whereas the tubulin stabilizer paclitaxel showed the expected enhancement in tubulin polymerization.

Immunocytochemistry. Incubation of human ovarian carcinoma cells with 200 nmol/L TubA led to a rounding up of cells and a concomitant depletion of microtubule structures (Supplementary Fig. S3). Tubulin staining seemed homogenous and the length of observable tubules was decreased. Untreated control cells showed a normal microtubule network

for interphase cells and several mitotic cells with what seem to be biopolar spindles were visible. In contrast, no mitotic cells or spindle formation was observed in the TubA-treated cells.

Tolerability. The MTD of TubA given i.v. in three weekly doses was found to be 0.05 mg/kg in non–tumor-bearing nude mice (Supplementary Table S4). Using the same schedule and route of administration, the MTD of CDP-TubA was found to be 6 mg/kg (TubA equivalents), an increase of approximately 100-fold over the small molecule analog. Doses above the MTD resulted in animal deaths that were preceded by body weight loss, with maximum body weight loss occurring usually on day 4, three days after the first dose or day 11, three days after second dose. At a dose of 6 mg/kg, a maximum weight loss of 10.8% was observed on day 4.

Efficacy in the human HT29 colon carcinoma xenografts. The antitumor activity of CDP-TubA was evaluated in s.c. HT29 human colon carcinoma xenografts established in female athymic nude mice (Fig. 2, Table 2).

There was no difference between untreated (data not shown) and vehicle-treated animals. This initial study was designed to compare the unconjugated TubA peptide and the CDP-TubA conjugate at equitoxic doses of approximately 50% of MTD based on tolerability determined in non–tumor-bearing nude mice. However, three weekly doses of Tub A at 0.1 mg/kg were found to be above the MTD in tumor-bearing mice, resulting in 50% mortality. The median TTE for the remaining mice was comparable with untreated animals.

In contrast, three weekly doses of CDP-TubA at 3 mg/kg were well tolerated with a body weight loss of 2.2% on day 4. This treatment resulted in a significant tumor growth delay (TGD) of 119%, three 90-day survivors, six partial regressions, and three complete regressions, with one tumor-free survivor.

The vinblastine and paclitaxel reference treatments resulted in TGDs of 127% and 34%, respectively. These results were statistically significant compared with vehicle treatment. Whereas treatment with vinblastine resulted in no regressions, paclitaxel induced two 90-day survivors, one partial regression, and nine complete regressions, with one tumor-free survivor. Treatment with weekly vinblastine was well tolerated; paclitaxel treatment resulted in a maximum group mean body weight loss of 10.2% indicating that it was dosed at its MTD. Two animals in the paclitaxel group displayed hind leg paralysis, a common side effect of this treatment.

Statistical analysis showed that weekly CDP-TubA at approximately 50% MTD was significantly more effective in both Kaplan-Meier survival as well as tumor size reduction compared with vinblastin at an equitoxic dose and as effective as paclitaxel at its MTD. A single dose of CDP-TubA at 3 mg/kg also showed significant antitumor activity resulting in TGD equivalent to and tumor size control superior to weekly vinblastine.

Efficacy in the human H460 non–small cell lung carcinoma xenografts. Efficacy was further evaluated in human H460 non–small cell lung carcinoma xenografts established s.c. in female nude mice (Fig. 3, Table 3). In order to enable comparison of efficacy at equitoxic doses in this second efficacy study, the dose of unconjugated TubA was reduced to 0.025 mg/kg (approx. 50% of MTD) and polymer-conjugated TubA was studied at both 3 and 6 mg/kg (approximately 50% and 100% of MTD), respectively.

There was no significant difference in tumor growth between untreated (data not shown) and vehicle-treated animals. In the untreated control group, however, one long-term survivor with a regressing tumor indicated a potential background of spontaneous tumor regression.

Treatment with tubulysin A resulted in a nonsignificant TGD and reduction in tumor burden on day 25, the time when tumors of control animals reached the predetermined average size of 2,000 mm^3. The vinblastine and paclitaxel reference treatments resulted in TGDs of 109% and 77%, respectively. Tumor sizes on day 25 were also reduced to 41% and 35% of vehicle controls, respectively. These results were statistically significant compared with vehicle treatment. One tumor-free survivor was reported in each of the reference groups, which may have been responses to treatment or spontaneous regressions. Mean body weight loss was more pronounced in the paclitaxel group (17.5%), indicating that it was dosed at the MTD, whereas the vinblastine group showed a body weight loss of 6.7%. Clinical observations of hind leg paralysis were recorded in all animals in the paclitaxel group but were not observed in any other treatment groups.

Treatment with CDP-TubA at 3 and 6 mg/kg resulted in a dose-dependent TGD of 113% and 158%, respectively. Average tumor sizes on day 25 were also reduced to 40% and 6.7% of vehicle controls, respectively. These results were statistically significant compared with vehicle controls. One tumor-free survivor was recorded in each of the CDP-TubA groups. Tumor growth curves indicate that CDP-TubA at 6 mg/m^2 resulted in tumor stasis for approximately two weeks after the final dose. CDP-TubA at 6 mg/m^2 also showed the smallest average tumor size of any treatment at day 25, a difference that was statistically significant compared with paclitaxel and with low-dose CDP-TubA but not with vinblastine. CDP-TubA treatments were well tolerated with a maximum body weight loss of 7.9% in the high-dose group.

Discussion

Microtubule-targeted agents such as the microtubule stabilizer paclitaxel or microtubule destabilizer vinblastine have gained significant clinical use. Despite their impressive clinical success, however, there remains room for improvement in a variety of areas such as (*a*) a broader spectrum of antitumor activity to include diseases not responsive to current tubulin inhibitors (e.g. colorectal cancer), (*b*) activity in previously treated, resistant tumors (e.g. taxane-resistant lung or ovarian cancer), (*c*) reduced toxicity, and (*d*) improved efficacy (i.e. survival). Tubulysins are microtubule-targeted, peptide-like compounds that have been shown to have many desirable characteristics suitable for a chemotherapeutic agent such as high potency in a wide variety of tumor cells, high activity in multidrug resistant cell lines including cells resistant to paclitaxel, high antiangiogenic activity, and lack of cytochrome P450 interaction. However, their potential as anticancer drugs is severely hampered by their low solubility and high toxicity. For instance, in our hands TubA had a MTD of 0.05 mg/kg in nude mice, which was significantly below the therapeutic dose in xenograft models. Tubulysins are therefore good candidates for targeted delivery to tumors. One way of achieving this is through the use of macromolecular carrier systems. CDP, a linear copolymer of β-cyclodextrin and polyethylene glycol, is a unique carrier for potent small molecule drugs because its conjugates self-assemble into nanoparticles with neutral surface

Table 3. Antitumor activity of CDP-TubA in the H460 human non–small cell lung carcinoma xenograft model in nude mice

Group	Treatment regimen			Median	T-C	%TGD	Statistical significance*		
	Agent	mg/kg	Schedule	TTE			vs G1	vs G5	vs G6
1	Vehicle	—	qwk ×3	20.3	—	—	—	‡	‡
2	Tubulysin	0.025	qwk ×3	23.7	3.4	17	ns	§	ns
3	Paclitaxel	30	qod ×5	35.9	15.6	77	‡	ns	ns
4	Vinblastine	8	qwk ×3	42.4	22.1	109	§	ns	ns
5	CDP-TubA	6	qwk ×3	52.3	32.0	158	‡	—	‖
6	CDP-TubA	3	qwk ×3	43.2	22.9	113	§	‖	—

NOTE: Potency was evaluated using log-rank testing on the time it took for individual tumors to reach a predetermined endpoint (TTE) of 2,000 mm^3 and by comparing the mean tumor volume (MTV) for different treatment groups when tumors of vehicle treated animals reached 2,000 mm^3 (day 25). Ten animals per group were treated. CDP-TubA (batch #2) doses are in tubulysin equivalents.
MTV, mean tumor volume ± SD (mm^3) on the day the vehicle control group mean tumor volume reached the predetermined endpoint of 2,000 mm^3.
*Statistical significance = Logrank test.
†Statistical significance = ANOVA w. Tukey's post test.
‡$P < 0.001$.
§$P < 0.01$.
‖$P < 0.05$.

charge and high solubility. This has been shown before for conjugates with camptothecin (20) and methylprednisolone (30) and again here in the case of TubA, in which an average particle size of around 100 nm was observed for conjugates whereas parent polymer had an average size of 8 nm by dynamic light scattering.

In addition to size, charge, and hydrophilicity, the choice of linker chemistry is important for successful tumor targeting. Ideally, the linker should show significant stability in circulation while allowing for the controlled release of active drug from the conjugate in the tumor, a characteristic that has been reported for disulfide linkers. Because TubA does not contain any thiol groups, this strategy required derivatization of the molecule. Recently, multiple, fully synthetic tubulysin analogs have successfully been synthesized, enabling the study of the structure-activity relationship of these compounds (1). Based on these results, we hypothesized that the introduction of a marcaptoethyl amide group at the carboxy-terminus of TubA may be possible without causing a significant loss of target inhibition and cytotoxicity. The primary mode of action of TubA is through potent inhibition of tubulin polymerization. In a cell-free system, 3 to 5 μmol/L TubA were able to inhibit polymerization of 30 μmol/L tubulin by 50%. Consistent with this mode of action, cancer cells exposed to TubA for a short period of time showed a loss of microtubule structures and a lack of spindle formation. The mercaptoethyl amide derivative TubA-SH remained a potent inhibitor of tubulin polymerization, being about 20% less active than TubA in the cell-free tubulin polymerization assay. The polymer conjugate of TubA-SH showed some effect on tubulin polymerization kinetics but not on the final extent of polymerization, indicating that release of tubulysin from the polymer is required for effective target inhibition. The kinetic effect was mediated by TubA, because a steroid conjugate at the same concentration had no effect on tubulin polymerization. Consistent with these results, the TubA-SH derivative also showed potent *in vitro* cytotoxicity in three different human tumor cell lines (IC_{50} of 4.4 to 19 nmol/L) and was only moderately less potent than the TubA parent molecule (1.3 to 2.8 nmol/L), confirming our initial hypothesis.

Release studies in PBS and human plasma confirmed that the disulfide-linked polymer conjugate was very stable under physiologic conditions. At the same time it retained its cytotoxic activity, indicating reduction of the disulfide linker and efficient release of active drug upon incubation with cells. We have previously shown that cyclodextrin-based polymers bind to tumor cells and get internalized efficiently into endosomes (29). Although the exact mechanism of disulfide reduction upon endocytosis is still under investigation, multiple studies have shown the efficiency of this process (for a review see ref. 24). For example, Yang et al. found that endocytosis through the folate receptor leads to rapid reduction of disulfide linkers with a half-life of 6 hours and that release was not dependent on the redox machinery associated with the cell surface (31). Arunachalam et al. identified a lysosomal thiol reductase in B cells that was capable of catalyzing disulfide bond reduction under low pH conditions (32). Feener et al. found that reduction of disulfide bonds was cell surface–mediated and not related to endosomes or lysosomes (33). On the other hand, the cleavage of certain internalized disulfide-based antibody-drug conjugates was found to be independent of the reducing potential in endosomes/lysosomes (34). Regardless of the exact mechanism of action, our data confirm that the release of the disulfide-linked tubulysin prodrug was a very efficient cellular process.

Polymer conjugation of TubA resulted in a dramatic 100-fold increase in MTD in nude mice, suggesting that the conjugate was stable in circulation *in vivo*. This increased tolerability translated into increased efficacy in two s.c. human cancer xenografts. Whereas TubA at its MTD was completely inactive, CDP-TubA showed equal or superior efficacy compared with vinblastine and paclitaxel reference treatments with minimal observed toxicity. In the H460 non–small cell lung carcinoma study, weekly CDP-TubA at its MTD was the most active treatment showing prolonged tumor growth suppression for up to 2 weeks after the last administration, suggesting efficient

Table 3. Antitumor activity of CDP-TubA in the H460 human non–small cell lung carcinoma xenograft model in nude mice (Cont'd)

MTV	Statistical significance †			Regressions			Mean BW	TR
Day 25	vs G1	vs G5	vs G6	PR	CR	TFS	Nadir	Deaths
2144 ± 454	—	‡	‡	0	0	0	—	0
1799 ± 834	ns	‡	‡	0	1	1	—	0
884 ± 388	‡	‖	ns	0	1	1	-17.5% Day 14	0
752 ± 563	‡	ns	ns	0	1	1	-6.7% Day 5	0
144 ± 74.7	‡	—	‖	0	1	1	-7.9% Day 3	0
847 ± 441	‡	‖	—	0	0	0	-0.4% Day 4	0

delivery of prodrug and prolonged release of active drug within the tumors. This is the first successful showing of antitumor activity against established tumors by a tubulysin analog *in vivo*. These observations confirm that cyclodextrin-based polymer conjugation through a disulfide linker is a valid approach to increasing the therapeutic index of tubulysins. Although more detailed pharmacokinetic and pharmacodynamic studies remain to be done, our results give hope that macromolecular prodrugs with intelligently designed linkers may enable the development of this class of compounds in diseases with high unmet medical need such as solid tumors refractory or resistant to current microtubule inhibitors.

Disclosure of Potential Conflicts of Interest

T. Schluep and J. Hwang are employed by and have an ownership interest in Calando Pharmaceuticals. G. Jensen has an ownership interest in Calando Pharmaceuticals. W. Richter is employed by and has an ownership interest in R&D Biopharmaceuticals. T. Schluep, P. Gunawan, L. Ma, G. Jensen, S. Hinton, J. Duringer, and J. Hwang are employed by Insert Therapeutics.

Acknowledgments

We thank Anna Avrutskaya, Robert Mullin at Piedmont Research Center (Morrisville, NC) for conducting all the subcutaneous tumor xenograft studies, and Ching-Jou Lim for experimental support and suggestions.

References

1. Wang Z, McPherson PA, Raccor BS, et al. Structure-activity and high-content imaging analyses of novel tubulysins. Chem Biol Drug Des 2007;70:75–86.
2. Wipf P, Wang Z. Total synthesis of N14-desacetoxytubulysin H. Org Lett 2007;9:1605–7.
3. Peltier HM, McMahon JP, Patterson AW, Ellman JA. The total synthesis of tubulysin D. J Am Chem Soc 2006;128:16018–9.
4. Domling A, Beck B, Eichelberger U, et al. Total synthesis of tubulysin U and V. Angew Chem Int Ed Engl 2006;45:7235–9.
5. Wipf P, Takada T, Rishel MJ. Synthesis of the tubuvaline-tubuphenylalanine (Tuv-Tup) fragment of tubulysin. Org Lett 2004;6:4057–60.
6. Höfle G, Glaser N, Leibold T, Karama U, Sasse F, Steinmetz H. Semisynthesis and degradation of the tubulin inhibitors epothilone and tubulysin. Pure Appl Chem 2003;75:167–78.
7. Kaur G, Hollingshead M, Holbeck S, et al. Biological evaluation of tubulysin A: a potential anticancer and antiangiogenic natural product. Biochem J 2006; 396:235–42.
8. Khalil MW, Sasse F, Lunsdorf H, Elnakady YA, Reichenbach H. Mechanism of action of tubulysin, an antimitotic peptide from myxobacteria. Chembiochem 2006;7:678–83.
9. Domling A, Richter W. Myxobacterial epothilones and tubulysins as promising anticancer agents. Mol Divers 2005;9:141–7.
10. Steinmetz H, Glaser N, Herdtweck E, Sasse F, Reichenbach H, Hofle G. Isolation, crystal and solution structure determination, and biosynthesis of tubulysins-powerful inhibitors of tubulin polymerization from myxobacteria. Angew Chem Int Ed Engl 2004;43: 4888–92.
11. Sandmann A, Sasse F, Muller R. Identification and analysis of the core biosynthetic machinery of tubulysin, a potent cytotoxin with potential anticancer activity. Chem Biol 2004;11:1071–9.
12. Sasse F, Steinmetz H, Heil J, Hofle G, Reichenbach H. Tubulysins, new cytostatic peptides from myxobacteria acting on microtubuli. Production, isolation, physico-chemical and biological properties. J Antibiot (Tokyo) 2000;53:879–85.
13. Patterson AW, Peltier HM, Ellman JA. Expedient synthesis of N-methyl tubulysin analogues with high cytotoxicity. J Org Chem 2008;73:4362–9.
14. Torchilin VP. Targeted pharmaceutical nanocarriers for cancer therapy and imaging. AAPS J 2007;9:E128–47.
15. Drummond DC, Meyer O, Hong K, Kirpotin DB, Papahadjopoulos D. Optimizing liposomes for delivery of chemotherapeutic agents to solid tumors. Pharmacol Rev 1999;51:691–743.
16. Reddy JA, Dorton R, Westrick E, et al. Preclinical evaluation of EC145, a folate-vinca alkaloid conjugate. Cancer Res 2007;67:4434–42.
17. Carter PJ, Senter PD. Antibody-drug conjugates for cancer therapy. Cancer J 2008;14:154–69.
18. Vicent MJ. Polymer-drug conjugates as modulators of cellular apoptosis. AAPS J 2007;9:E200–7.
19. Duncan R, Vicent MJ, Greco F, Nicholson RI. Polymer-drug conjugates: towards a novel approach for the treatment of endrocine-related cancer. Endocr Relat Cancer 2005;12:S189–99.
20. Cheng J, Khin KT, Jensen GS, Liu A, Davis ME. Synthesis of linear, β-cyclodextrin-based polymers and their camptothecin conjugates. Bioconjug Chem 2003;14:1007–17.
21. Schluep T, Hwang J, Cheng J, et al. Preclinical efficacy of the camptothecin-polymer conjugate IT-101 in multiple cancer models. Clin Cancer Res 2006;12:1606–14.
22. Schluep T, Cheng J, Khin KT, Davis ME. Pharmacokinetics and biodistribution of the camptothecin-polymer conjugate IT-101 in rats and tumor-bearing mice. Cancer Chemother Pharmacol 2006;57:654–62.
23. Oliver CJ, Yen Y, Synold T, Schluep T, Davis ME. A dose-finding pharmacokinetic study of IT-101, the first de novo designed nanoparticle therapeutic, in refractory solid tumors. J Clin Oncol (Meeting Abstracts) 2008;26:14538.
24. Saito G, Swanson JA, Lee KD. Drug delivery strategy utilizing conjugation via reversible disulfide linkages: role and site of cellular reducing activities. Adv Drug Deliv Rev 2003;55:199–215.
25. Chen Q, Millar HJ, McCabe FL, et al. αv integrin-targeted immunoconjugates regress established human tumors in xenograft models. Clin Cancer Res 2007;13:3689–95.
26. Erickson HK, Park PU, Widdison WC, et al. Antibody-maytansinoid conjugates are activated in targeted cancer cells by lysosomal degradation and linker-dependent intracellular processing. Cancer Res 2006;66:4426–33.
27. Griffiths GL, Mattes MJ, Stein R, et al. Cure of SCID mice bearing human B-lymphoma xenografts by an anti-CD74 antibody-anthracycline drug conjugate. Clin Cancer Res 2003;9:6567–71.
28. Chari RV. Targeted cancer therapy: conferring specificity to cytotoxic drugs. Acc Chem Res 2008;41: 98–107.
29. Cheng J, Khin KT, Davis ME. Antitumor activity of b-cyclodextrin polymer-campthothecin conjugates. Mol Pharm 2004;1:183–93.
30. Hwang J, Rodgers K, Oliver CJ, Schluep T. a-Methylprednisolone conjugated cyclodextrin polymer-based nanoparticles for rheumatoid arthritis therapy. Int J Nanomedicine 2008;3:359–71. Epub 2008 Jun 26.
31. Yang J, Chen H, Vlahov IR, Cheng JX, Low PS. Evaluation of disulfide reduction during receptor-mediated endocytosis by using FRET imaging. Proc Natl Acad Sci U S A 2006;103:13872–7.
32. Arunachalam B, Phan UT, Geuze HJ, Cresswell P. Enzymatic reduction of disulfide bonds in lysosomes: characterization of a γ-interferon-inducible lysosomal thiol reductase (GILT). Proc Natl Acad Sci U S A 2000;97:745–50.
33. Feener EP, Shen WC, Ryser HJ. Cleavage of disulfide bonds in endocytosed macromolecules. A processing not associated with lysosomes or endosomes. J Biol Chem 1990;265:18780–5.
34. Austin CD, Wen X, Gazzard L, Nelson C, Scheller RH, Scales SJ. Oxidizing potential of endosomes and lysosomes limits intracellular cleavage of disulfide-based antibody-drug conjugates. Proc Natl Acad Sci U S A 2005;102:17987–92.

Clinical Cancer Research

Polymeric Tubulysin-Peptide Nanoparticles with Potent Antitumor Activity

Thomas Schluep, Paula Gunawan, Ling Ma, et al.

Clin Cancer Res 2009;15:181-189.